Femtosecond Probing of Plasma Wakefields and Observation of the Plasma Wake Reversal Using a Relativistic Electron Bunch

C. J. Zhang, J. F. Hua, Y. Wan, C.-H. Pai, B. Guo, J. Zhang, Y. Ma, F. Li, Y. P. Wu, H.-H. Chu, Y. Q. Gu, X. L. Xu, W. B. Mori, C. Joshi, J. Wang, and W. Lu

Phys. Rev. Lett. **119**, 064801 — Published 9 August 2017

DOI: 10.1103/PhysRevLett.119.064801

Femtosecond probing of plasma wakefields and observation of the plasma wake reversal using a relativistic electron bunch

C. J. Zhang,[1] J. F. Hua,[1] Y. Wan,[1] C.-H. Pai,[1] B. Guo,[1] J. Zhang,[1] Y. Ma,[1] F. Li,[1] Y. P. Wu,[1] H.-H. Chu,[2] Y. Q. Gu,[3] X. L. Xu,[4] W. B. Mori,[4] C. Joshi,[4] J. Wang,[2,5,6,*] and W. Lu[1,7,†]

[1] *Department of Engineering Physics, Tsinghua University, Beijing 100084, China*
[2] *Department of Physics, National Central University, Jhong-Li 32001, Taiwan*
[3] *Science and Technology on Plasma Physics Laboratory, Laser Fusion Research Center, CAEP, Mianyang 621900, China*
[4] *University of California Los Angeles, Los Angeles, California 90095, USA*
[5] *Institute of Atomic and Molecular Sciences, Academia Sinica, Taipei 10617, Taiwan*
[6] *Department of Physics, National Taiwan University, Taipei 10617, Taiwan*
[7] *IFSA Collaborative Center, Shanghai Jiao Tong University, Shanghai 200240, China*

(Dated: June 2, 2017)

We show that a high-energy electron bunch can be used to capture the instantaneous longitudinal and transverse field structures of the highly transient, microscopic, laser-excited relativistic wake with femtosecond resolution. The spatio-temporal evolution of wakefields in a plasma density up-ramp is measured and the reversal of the plasma wake, where the wake wavelength at a particular point in space increases until the wake disappears completely only to reappear at a later time but propagating in the opposite direction, is observed for the first time by using this new technique.

Relativistic wakes produced by intense laser or charged particle beams propagating through plasmas are being considered as accelerators[1, 2] for next generation of colliders[3] and coherent light sources[4]. The phase velocity of the wake is nearly the speed of light c and the longitudinal electric field can be orders of magnitude larger than that in conventional accelerators[1, 2]. Such wakes in uniform density plasmas have been shown to accelerate electrons and positrons to several gigaelectronvolts (GeV)[5–11], with a few percent energy spread[9–11] and a high wake-to-beam energy transfer efficiency[8]. To optimize both the efficiency and the energy spread of the accelerated beam, accurate information about the field structure of the wake is needed. This is difficult because the wakes are microscopic, highly transient and relativistic. Also wakes in density gradients are important for controlled injection[12, 13] and alleviating dephasing[14].

In previous studies, optical methods such as frequency domain interferometry[15], Faraday rotation effect[16, 17] and ultrafast shadowgraphy[17, 18] were used to diagnose the dimensions and shape of the wake in high-density plasmas. Recently the transverse oscillations of the drive electron beam itself were used to give spatially integrated information about the longitudinal variation of the fields of a highly nonlinear wake[19]. Although low-energy proton and electron beams have been used to study the transient fields in laser-produced plasmas[20, 21], they are not suitable for capturing relativistic plasma wakes. Electron beams generated from a laser wakefield accelerator (LWFA) were also used to detect the transient magnetic fields[22] in laser-produced plasmas. No technique to-date has given instantaneous information about both the transverse and longitudinal distribution of the electric field of the wake. This is especially true of linear (sinusoidal) plasma wakes produced in low-density plasmas that can accelerate both electrons and positrons for an electron-positron collider[3].

An ultra-short, high-energy electron bunch is ideal for quantitatively mapping the wakefield directly, since electrons can be deflected by the electric field. To diagnose the high-gradient wakes propagating at speed of light c requires the probe electrons to have high enough energy ($\gamma \gg 1$), and its duration τ to be much smaller than a plasma period ($\tau \ll \lambda_p/c$), which turns out to be a few (tens of) fs for a $10^{19}(10^{17})$ cm^{-3} plasma. Electron bunches generated from a laser wakefield accelerator meet both of these requirements.

In this letter, we demonstrate for the first time that the electric fields of a linear wake produced in a plasma with density as low as 10^{17} cm^{-3} can be accurately mapped in a single shot using an ultrashort, high-energy bunch of electrons generated by a LWFA. Such low-density plasmas will be needed for building a single-stage 10 GeV LWFA[23]. Furthermore, we have probed the structure of wakefields in a density gradient for the first time. By using this technique, a reversal of the plasma wake in a density up-ramp is discovered.

The schematic of the concept is illustrated in Fig.1. The experiments were carried out using the 100-TW laser platform at National Central University, Taiwan[24]. The relativistic electron beam is generated by focusing a 25-TW, 40 fs (full width at half maximum, FWHM), Ti-sapphire laser pulse to give a peak normalized vector potential $a_0 = 2.0$ into a 8×10^{18} cm^{-3} density plasma produced using a gas mixture of 95% helium and 5% nitrogen. The laser pulse excites a highly nonlinear wake and accelerates ionization injected[25] electrons. The peak energy of the probe beam fluctuates shot by shot between 60-80 MeV with an 15-MeV energy spread. The

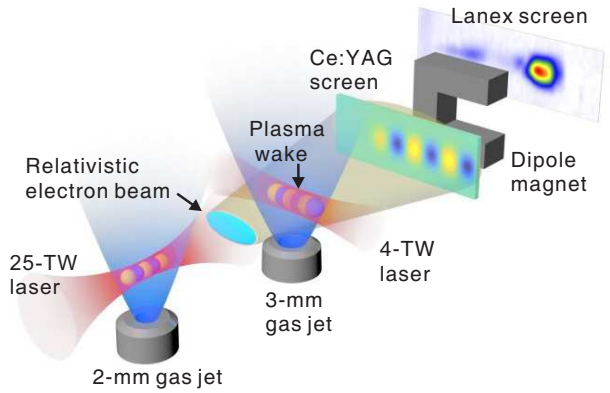

FIG. 1. The schematic drawing of the probing of a laser-driven plasma wakefield using a relativistic electron beam.

charge contained in the mono-energetic peak varies between 2-10 pC. The divergence of the probe is 2 mrad (root-mean-square, rms). The pulse length of the probe is measured to be 1-3 fs rms[26].

After propagating through free space for 11 cm, the probe beam intercepts at right angle a second weaker/linear wake produced by a 4-TW, 100-fs, $a_0 = 0.26$ Ti-sapphire laser in a variable density helium plasma. Both plasmas are produced by ionization of the gas emanating from supersonic gas jet nozzles with a diameter of 2 mm (probe beam) and 3 mm (wake to be probed). As the electron probe traverses the wake being probed, some of the electrons are deflected by the intense electric field in the wake. These deflections, which originally appear as transverse momentum modulations of the probe beam, evolve into density modulations. The density modulated probe is detected by recording the visible light produced by the beam impinging upon a 100 μm thick cerium-doped yttrium aluminum garnet (Ce:YAG) screen placed 11-42 cm downstream from the second nozzle. The inherent resolution of the Ce:YAG screen is about 7 μm. The visible light is collected and transmitted by a relay imaging system with a magnification of 2.5 and a spatial resolution of 2.8 μm, then recorded by an electron multiplying charge coupled device (EMCCD). A 30-μm thick aluminum foil is placed in front of the Ce:YAG screen to block the residual laser light and X-rays from betatron radiation. The imaging system can be removed online so that the electron bunch can be characterized.

An example of wakefield snapshots is shown in Fig. 2(a), with the position of the laser marked by the dashed circle. Using this data, the density modulation of the probe beam, $\delta n/n_0 = (n - n_0)/n_0$ is derived and shown in Fig. 2(b). Here n is the measured probe density, n_0 is the corresponding background, which is obtained by smoothing the data to remove the modulation induced by the wakefield.

Useful information of the wake being probed, such as

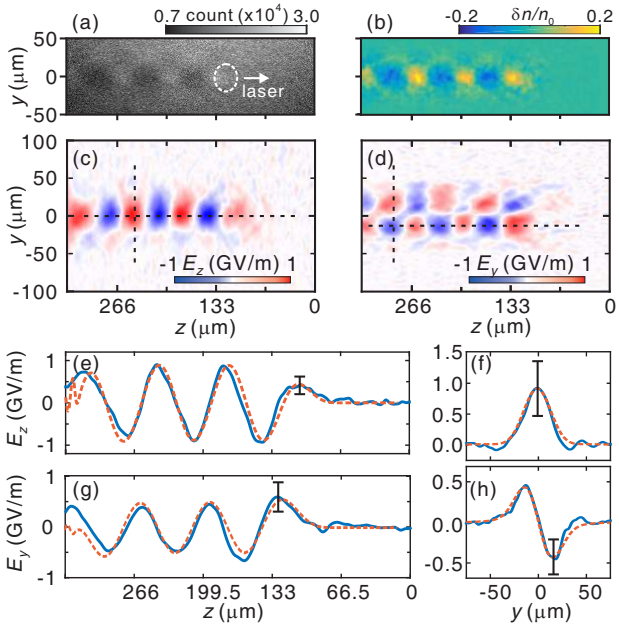

FIG. 2. Snapshot of the wake, the deduced electric field structure of the wake and comparison with simulations. (a), Raw image of the probe density n. (b), Density modulation $\delta n/n_0$. (c) and (d), The (y, z) plot of the reconstructed E_z and E_y field respectively. (e) and (f), The axial and transverse ($z = 242$ μm) lineouts of E_z respectively. (g) and (h), the axial (at $y = -10$ μm) and transverse ($z = 300$ μm) lineouts of E_y. The blue solid lines show the experimental data, while the red dashed lines are from simulations. The transverse lineouts are taken at positions where the agreement between the simulations and the experiment is the closest. The error bars arise from the fluctuating energy, pulse width and correlated divergence of the probe beam.

the shape and dimensions can be directly obtained from the snapshots in Figs. 2(a) and (b). For example, the wavelength of the wake is 65 μm, indicating a plasma density as low as 3×10^{17} cm^{-3}. The radius of the wake is about 10 μm (rms), corresponding to approximate one collisionless skin depth of the plasma. The transit time of the probe through the wake is 66 fs. However, the time resolution is mainly determined by the length of the probe beam (1-3 fs rms) for a linear wake as explained in [27].

Linear wakes are almost completely electrostatic thus the contribution of magnetic fields is negligible. Therefore the density modulation $\delta n/n_0$ is related to the electric field $E_{x,y,z}$ of the wake by[27],

$$\frac{\delta n}{n_0} = \frac{K_\tau K_E K_\theta}{M} \frac{eL}{\beta c p_0} \nabla \cdot \int_{-s}^{s} E(x, y, z - \beta_E x) dx \quad (1)$$

where the limits of integration $\pm s$ should be large enough to cover the transverse extent of the wakefield. Here the wake propagates along the z direction at a speed of $\beta_E c$ and the probe traverses along the x direction; $p_0 = \gamma m_e c$ is the central momentum of the probe beam, γ is the

Lorentz factor, e the electron charge, βc the velocity of the probe, L the drift distance in vacuum, M the geometric magnification and K_τ, K_E and K_θ are correction factors for pulse length, energy spread and correlated divergence angle of the probe beam. For the plasma and probe parameters used in this experiment, $K_\tau \approx 1$, $K_E \approx 1$ and $K_\theta \approx 0.3$ (see Supplementary Material section 1, SM1 for details).

The reconstructed fields are shown in Figs. 2(c) and (d), for the longitudinal E_z and transverse E_y component of the electric field respectively. To make a quantitative comparison, we take axial and radial lineouts of the longitudinal and transverse fields as shown in Figs. 2(e) through (h). Since the laser is weak ($a_0 = 0.26$) and has a near Gaussian profile, the wake being probed is quasi-linear and therefore the longitudinal field is expected to have a near-sinusoidal form along the z direction and a Gaussian form along the y direction[28] as seen in the blue experimental curves in Figs. 2(e) and (f). Furthermore $E_z(y,z)$ obtained from the particle-in-cell (PIC) simulation using Osiris[29] (red dashed lines) fit both the observed longitudinal and transverse variations of the measured E_z very well. Note that the simulation used an $a_0 = 0.22$ to account for the non-ideal laser focal spot in the experiment (see SM2 for the details of the simulations). Figures 2(g) and (f) show the reconstructed longitudinal and transverse variations of the E_y field. In the longitudinal direction, the E_y field is $\pi/2$ out of phase with the E_z field as expected for a linear wake[28]. Meanwhile, the transverse variation of the E_y field is of the form $ye^{-y^2/2\sigma^2}$, also in excellent agreement with the measured E_y field. The peak accelerating field is 0.9 ± 0.4 GeV/m, in good agreement with simulations. Moreover, the transverse field is approximately linear over ± 8 μm. This linear portion is critical for preserving the emittance of the accelerating electrons. Although the wake measured in this experiment is in the linear regime, this probing technique can be extended to give qualitative features of highly nonlinear wakes[27].

We now show applications of this technique and new phenomena it has uncovered. First, it is used to characterize the density ramp of a low-density gas jet that is otherwise extremely hard to diagnose. Second, by recording the temporal evolution of the plasma wake at one z location in a density up-ramp, we have observed that the wavenumber of the wake at a particular position at first decreases until the wake disappears completely only to reappear at a later time with its phase velocity reversed and its wavenumber now monotonically increases with time.

Figure 3(a) shows the axial lineouts of modulated probe density for different time delays. For these measurements, the distance between the source of the probe and the probed wake is 11 cm so only 500 μm region of the wake could be recorded at any one time and the angular jitter of the probe beam is advantageously used to capture the location of the laser pulse at different delay times by taking a large number of shots. The wake propagates from left to right through the density up-ramp. The centers of the first wake period for each time delay are marked by blue dots. Since the wake trails the laser pulse that excites it, the slope of positions of these blue dots gives the phase velocity of the wake to be the speed of light as expected.

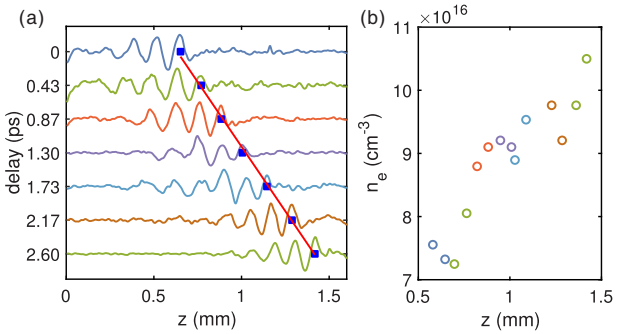

FIG. 3. (a) Propagation of wakefield in an increasing plasma density ramp. Different lines correspond to the axial lineout of density modulation of the probe at different times. The blue dots mark the center of the first wake period and is fitted by the red line with a slope $dz/dt = c$ confirming that it is also the position of the wake-driving laser pulse. (b) The retrieved initial density profile of the plasma density up-ramp of the gas jet seen by the laser pulse using data in (a). Color tables in (a) and (b) are the same. The spread in data is indicative of the shot-to-shot reproducibility of the gas jet density profile.

The wavelength of the wake shown in Fig. 3(a) can be used to retrieve the initial density profile of the plasma up-ramp. For the first period of the wake just behind the laser, the wavelength of the wake is determined by the initial plasma density through $\lambda_p(z) = 2\pi c(e^2 n_e/\epsilon_0 m_e)^{-1/2}$, since there is not enough time for the wake to evolve.

The retrieved initial plasma density profile is shown in Fig. 3(b). As can be seen, the plasma density increases from 7×10^{16} cm^{-3} to 1.1×10^{17} cm^{-3} in 900 μm. These densities are too low to be measured by the frequently-used interferometer technique. This new diagnostic tool gives the ability to characterize such low-density up-ramps, seen by the laser pulse that actually excites the wake. This is important because in order to maximize the charge throughput and minimize the emittance growth, the accelerating bunch must be carefully matched from one plasma accelerator stage to the next. This can be done in principle by employing appropriately designed plasma density ramps at the entrance to and the exit from the plasma acceleration section to properly increase/decrease the focusing force acting on the electrons[30, 31]. Wakes produced in plasma density up-ramps may also be useful for overcoming the dephasing[14] thereby increasing the acceleration length to match the pump depletion length[32] of the laser

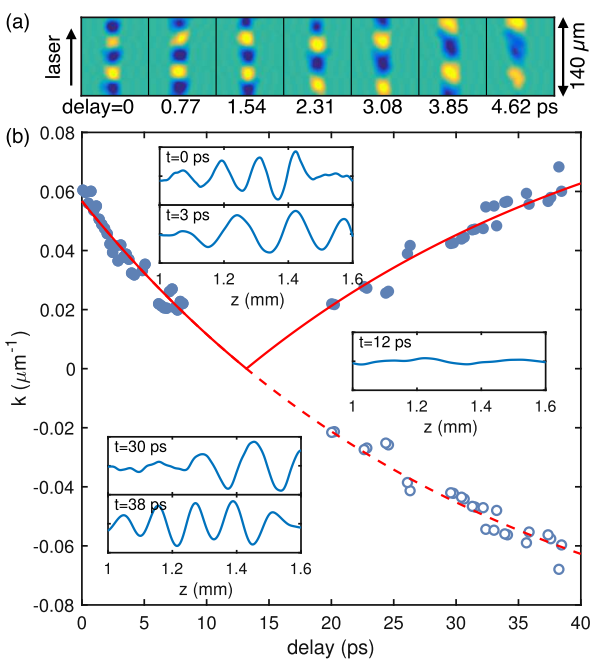

FIG. 4. (a) Experimental wakefield snapshots at different time delays at a particular z location with a range of $\Delta z = 140$ μm for $0 < t(\text{ps}) < 4.6$. The color tables in all the shots have been adjusted to highlight the wake wavelength variation. (b) Evolution of wakefield wave number k versus time over the (detectable) lifetime of the wake for a lower density plasma up-ramp than in (a). The blue dots are experimental measurements and the red solid line is the best fit to the data. The open circles and red dashed line are reflections of the measurements and fitting curve in the time region where k becomes negative. The axial lineouts of the wakefield amplitude (in arbitrary units) for five different time delays are shown in the insets.

pulse thereby increasing the energy transfer efficiency of a LWFA. On the other hand, density down-ramps have been suggested for controllable injection of charge into the wake[12, 13].

The reversal of the plasma wake in a density up-ramp is observed for the first time by recording the temporal evolution of the wake within a small window about one z position as shown in Fig. 4(a). One can see that the wake wavelength λ increases with time in a density up-ramp. This increase is not just attributable to plasma expansion[33] which occurs over a longer timescale but instead can be explained as follows. First, we note that a cold plasma wake has zero group velocity and continues to oscillate at its local plasma frequency $\omega_p(z)$ after the laser pulse has passed. The phase of the wave is given by $\phi = \omega_p(z)(t - z/v_d)$ where $v_d \approx c$ is the velocity of the drive laser pulse (the dependence of v_d on $\omega_p(z)$ is a higher order effect). Therefore, $\omega(z,t) \equiv \partial\phi/\partial t = \omega_p(z)$ and $k(z,t) \equiv -\partial\phi/\partial z = k_p(z) - \frac{\partial\omega_p}{\partial z}t$. This relationship implies that the wavenumber evolves in time according to $\partial k/\partial t = -\partial\omega_p/\partial z$[34]. For the up-ramp case, $\partial\omega_p/\partial z > 0$, which means $\partial k/\partial t < 0$ therefore the wavenumber of the wake will initially decrease with time. For planar (1D) wakes, this happens because the neighboring electron sheets dephase in such a way that the local wavelength of the wake first increases until it eventually tends towards infinity. After this time, the wavelength of the wake begins to shorten and the phase velocity of the wake reverses its direction. The wake wavelength now continues to shrink until the wake can eventually be damped by wave-particle interactions[35]. We call this phenomenon wake reversal.

We show the experimental verification of this reversal phenomenon in Fig. 4(b). The blue dots are experimental measurements of the wavenumber of the wake at different times for $1.3 < z(\text{mm}) < 1.5$. We can clearly see that the wavenumber between $0 < t(\text{ps}) < 8$ first decreases. Between $8 < t(\text{ps}) < 20$ no wake is observed. However, after this time the wake reappears and now its wavenumber increases with time. The red line is an exponentially decreasing function fit to all the data. The open circles and the dashed line are reflections of the corresponding data (since theory has $-k$ increasing) after the wake has reappeared. The insets in Fig. 4 show examples of the actual measurement of the wake at 5 representative times. Both the dots and the insets in Fig. 4(b) clearly show the disappearance and reappearance of the wake at a later time, namely, the reversal. In our shot-by-shot experiment the direction of the phase velocity of the wake cannot be determined. Nevertheless, according to theory the wavenumber of the wake should become negative after the wake wavenumber goes to zero.

Plasma expansion cannot explain the observed evolution of k in Fig. 4. If the wavenumber evolves only due to the density drop as a result of plasma expansion, it will monotonically decrease to zero and never increase again at a later time. However the best fit to the data shows a deviation from a linear decrease in k with time as might be expected if plasma density gradient $\partial\omega_p/\partial z$ were independent of time, indicating that the expansion of the plasma does play some role in reducing the local density gradient $\partial\omega_p(t)/\partial z|_z$ over the 40 ps time window.

This wake reversal only occurs in a density up-ramp. For the down-ramp case, $\partial k/\partial t > 0$, which means the wake wavenumber at a specific position monotonically increases as a function of time, therefore no reversal can appear. Because the peak a_0 of the initially unmatched laser pulse had become smaller due to diffraction and pump depletion[36] after propagating through a 3 mm plasma, no clear wakefield snapshots could be obtained to show the wake evolution in the down-ramp. However, both the existence of wake reversal in a density up-ramp and its absence in a density down-ramp are confirmed in PIC simulations (see SM3).

In conclusion, we have demonstrated the imaging of a relativistic plasma wake with femtosecond resolution

and the reconstruction of its field structure by utilizing an ultra-short relativistic electron probe. A new phenomenon of wake reversal in a plasma density up-ramp is observed. Such complete information obtained in the experiments is vital to the development of plasma based wakefield accelerators.

This work was supported by NSFC Grant No. 11425521, No. 11375006, No. 11535006, No. 11475101, the National Basic Research Program of China No. 2013CBA01501, the Thousand Young Talents Program, the Foundation of CAEP No. 2014A0102003, the Science Challenge Program Grant No. TZ2016005, the U.S. DOE Grant No. DE-SC0010064, No. DE-SC0008491, No. DE-SC0008316, No. DE-SC0014260, the U.S. NSF Grant PHY-1415386, No. ACI-1339893 and No. PHY-500630, and the Ministry of Science and Technology of Taiwan under Contracts No. 104-2112-M-001 -030 MY3. Simulations are performed on Hoffman cluster at UCLA and Hopper, Edison cluster at National Energy Research Scientific Computing Center (NERSC). The authors thank Dr. Te-Sheng Hung, Mr. Ying-Li Chang, Mr. Yau-Hsin Hsieh and Mr. Chen-Kang Huang for helping these experiments.

* jwang@ltl.iams.sinica.edu.tw
† weilu@tsinghua.edu.cn

[1] T. Tajima and J.M. Dawson, Physical Review Letters **43**, 267 (1979).
[2] P. Chen, J.M. Dawson, R. W. Huff, and T. Katsouleas, Physical review letters **54**, 693 (1985).
[3] C. Schroeder, E. Esarey, C. Geddes, C. Benedetti, and W. Leemans, Physical Review Special Topics-Accelerators and Beams **13**, 101301 (2010).
[4] S. Corde, K. T. Phuoc, G. Lambert, R. Fitour, V. Malka, A. Rousse, A. Beck, and E. Lefebvre, Reviews of Modern Physics **85**, 1 (2013).
[5] M. Hogan, C. Barnes, C. Clayton, F. Decker, S. Deng, P. Emma, C. Huang, R. Iverson, D. Johnson, C. Joshi, *et al.*, Physical review letters **95**, 054802 (2005).
[6] I. Blumenfeld, C. E. Clayton, F.-J. Decker, M. J. Hogan, C. Huang, R. Ischebeck, R. Iverson, C. Joshi, T. Katsouleas, N. Kirby, *et al.*, Nature **445**, 741 (2007).
[7] H. T. Kim, K. H. Pae, H. J. Cha, I. J. Kim, T. J. Yu, J. H. Sung, S. K. Lee, T. M. Jeong, and J. Lee, Physical review letters **111**, 165002 (2013).
[8] M. Litos, E. Adli, W. An, C. Clarke, C. Clayton, S. Corde, J. Delahaye, R. England, A. Fisher, J. Frederico, *et al.*, Nature **515**, 92 (2014).
[9] S. Corde, E. Adli, J. Allen, W. An, C. Clarke, C. Clayton, J. Delahaye, J. Frederico, S. Gessner, S. Green, *et al.*, Nature **524**, 442 (2015).
[10] X. Wang, R. Zgadzaj, N. Fazel, Z. Li, S. Yi, X. Zhang, W. Henderson, Y.-Y. Chang, R. Korzekwa, H.-E. Tsai, *et al.*, Nature communications **4** (2013).
[11] W. Leemans, A. Gonsalves, H.-S. Mao, K. Nakamura, C. Benedetti, C. Schroeder, C. Tóth, J. Daniels, D. Mittelberger, S. Bulanov, *et al.*, Physical review letters **113**, 245002 (2014).
[12] H. Suk, N. Barov, J. B. Rosenzweig, and E. Esarey, Physical review letters **86**, 1011 (2001).
[13] C.G.R. Geddes, K. Nakamura, G.R. Plateau, C. Toth, E. Cormier-Michel, E. Esarey, C.B. Schroeder, J.R. Cary, and W.P. Leemans, Physical review letters **100**, 215004 (2008).
[14] T. Katsouleas, Physical Review A **33**, 2056 (1986).
[15] N. H. Matlis, S. Reed, S. S. Bulanov, V. Chvykov, G. Kalintchenko, T. Matsuoka, P. Rousseau, V. Yanovsky, A. Maksimchuk, S. Kalmykov, *et al.*, Nature Physics **2**, 749 (2006).
[16] M.C. Kaluza, H.-P. Schlenvoigt, S.P.D. Mangles, A.G.R. Thomas, A.E. Dangor, H. Schwoerer, W.B. Mori, Z. Najmudin, and K.M. Krushelnick, Physical review letters **105**, 115002 (2010).
[17] A. Buck, M. Nicolai, K. Schmid, C. M. Sears, A. Sävert, J. M. Mikhailova, F. Krausz, M. C. Kaluza, and L. Veisz, Nature Physics **7**, 543 (2011).
[18] A. Sävert, S. Mangles, M. Schnell, E. Siminos, J. Cole, M. Leier, M. Reuter, M. Schwab, M. Möller, K. Poder, *et al.*, Physical review letters **115**, 055002 (2015).
[19] C. Clayton, E. Adli, J. Allen, W. An, C. Clarke, S. Corde, J. Frederico, S. Gessner, S. Green, M. Hogan, *et al.*, Nature communications **7** (2016).
[20] C. Li, F. Séguin, J. Frenje, M. Rosenberg, R. Petrasso, P. Amendt, J. Koch, O. Landen, H. Park, H. Robey, *et al.*, Science **327**, 1231 (2010).
[21] M. Centurion, P. Reckenthaeler, S. A. Trushin, F. Krausz, and E. E. Fill, Nature Photonics **2**, 315 (2008).
[22] W. Schumaker, N. Nakanii, C. McGuffey, C. Zulick, V. Chyvkov, F. Dollar, H. Habara, G. Kalintchenko, A. Maksimchuk, K. Tanaka, *et al.*, Physical review letters **110**, 015003 (2013).
[23] W. Lu, M. Tzoufras, C. Joshi, F. Tsung, W. Mori, J. Vieira, R. Fonseca, and L. Silva, Physical Review Special Topics-Accelerators and Beams **10**, 061301 (2007).
[24] T.-S. Hung, C.-H. Yang, J. Wang, S.-y. Chen, J.-Y. Lin, and H.-h. Chu, Applied Physics B **117**, 1189 (2014).
[25] A. Pak, K.A. Marsh, S.F. Martins, W. Lu, W.B. Mori, and C. Joshi, Physical Review Letters **104**, 025003 (2010).
[26] C. Zhang, J. Hua, Y. Wan, B. Guo, C.-H. Pai, Y. Wu, F. Li, H.-H. Chu, Y. Gu, W. Mori, *et al.*, Physical Review Accelerators and Beams **19**, 062802 (2016).
[27] C. Zhang, J. Hua, X. Xu, F. Li, C.-H. Pai, Y. Wan, Y. Wu, Y. Gu, W. Mori, C. Joshi, *et al.*, Scientific Reports **6** (2016).
[28] E. Esarey, C. Schroeder, and W. Leemans, Reviews of Modern Physics **81**, 1229 (2009).
[29] R. Fonseca, L. Silva, F. Tsung, V. Decyk, W. Lu, C. Ren, W. Mori, S. Deng, S. Lee, T. Katsouleas, *et al.*, "Osiris: a three-dimensional, fully relativistic particle in cell code for modeling plasma based accelerators," (Springer, 2002) pp. 342–351.
[30] T. Mehrling, J. Grebenyuk, F. Tsung, K. Floettmann, and J. Osterhoff, Physical Review Special Topics-Accelerators and Beams **15**, 111303 (2012).
[31] X. Xu, J. Hua, Y. Wu, C. Zhang, F. Li, Y. Wan, C.-H. Pai, W. Lu, W. An, P. Yu, *et al.*, Physical review letters **116**, 124801 (2016).
[32] W. Horton and T. Tajima, Physical Review A **34**, 4110 (1986).

[33] C. Joshi, C. E. Clayton, and F. F. Chen, Physical Review Letters **48**, 874 (1982).
[34] G. B. Whitham, *Linear and nonlinear waves*, Vol. 42 (John Wiley & Sons, 2011).
[35] J. Dawson, The Physics of Fluids **4**, 869 (1961).
[36] J.E. Ralph, K.A. Marsh, A.E. Pak, W. Lu, C.E. Clayton, F. Fang, W.B. Mori, and C. Joshi, Physical review letters **102**, 175003 (2009).